Journal of Nuclear Materials 415 (2011) 367–377

Contents lists available at ScienceDirect

Journal of Nuclear Materials

journal homepage: www.elsevier.com/locate/jnucmat

# Experience from the post-test analysis of MEGAPIE

L. Zanini [a,*], S. Dementjev [a], F. Gröschel [a], W. Leung [a], R. Milenkovic [a], K. Thomsen [a], W. Wagner [a], M. Wohlmuther [a], Xu Cheng [b], A. Class [b], A. Konobeyev [b], P. Agostini [c], P. Meloni [c], J.-C. David [d], A. Letourneau [d], S. Leray [d], S. Panebianco [d], L. Cachon [e], C. Latgé [e], P. Roubin [e], A. Guertin [f], N. Thiolliere [f], M. Dierckx [g]

[a] *Paul Scherrer Institut, 5232 Villigen PSI, Switzerland*
[b] *Institut für Neutronenphysik und Reaktortechnik, Karlsruher Institut für Technologie, Postfach 3640, 76021 Karlsruhe, Germany*
[c] *Ente per le nuove Tecnologie, l'Energia e l'Ambiente, Località Brasimone, 40032 Camugnano, Bologna, Italy*
[d] *CEA – Saclay, Irfu/Service de Physique Nucléaire, F91191 Gif-sur-Yvette, France*
[e] *CEA, Centre de Cadarache, DEN/DTN/DIR, F-13108 Saint Paul Lez Durance, France*
[f] *SUBATECH, EMN-IN2P3/CNRS-Université, Nantes, F-44307, France*
[g] *Studiecentrum voor Kernenergie/Centre d'Etude de l'Energie Nucléaire, Boeretang 200, 2400 Mol, Belgium*

ARTICLE INFO

*Article history:*
Available online 27 April 2011

ABSTRACT

The (MEGAWatt Pilot Experiment) MEGAPIE target was successfully irradiated in 2006 at the SINQ facility of the Paul Scherrer Institut. During the irradiation a series of measurements to monitor the operation of the target, the thermal hydraulics behavior and the neutronic and nuclear aspects, has been performed. In the post-test analysis phase of the project, the data were analyzed and important information relevant to accelerator-driven systems (ADS) was gained, in particular: (i) from the operation of the target several recommendations concern the simplification of the system and the improved reliability; (ii) data from the thermal hydraulic measurements have offered the opportunity to validate the codes used in the design phase; (iii) the neutronic analysis confirm the high performance of a liquid metal target and the importance of the delayed neutron measurements in an ADS target; (iv) the nuclear measurements of the gas released gave the opportunity to validate the codes used during the design phase and provided indications for the operation. From the results in these different domains recommendations to further development of ADS and heavy liquid metal targets are discussed.



## 1. Introduction

The spallation target is one of the most delicate and technically challenging components of an accelerator-driven system (ADS). The target and, if that option is chosen, its window are subjected to unusual stress, corrosion and irradiation conditions during steady state irradiation and transients. The MEGAPIE project has been the first experiment meant to design, manufacture, test, commission, operate and dismount a liquid metal spallation target at the MW beam power level [1]. The design phase of the project was supported by a R&D work divided in several areas, and performed by specialists from the corresponding research fields, studying problems related to thermal–hydraulics, structural mechanics, materials issues, neutronic and nuclear assessment.

A major milestone in the MEGAPIE project was achieved with the irradiation in 2006 at the SINQ facility of the Paul Scherrer Institut. During irradiation, a series of measurements concerning control, thermal–hydraulics, structural mechanics, neutronic and nuclear aspects were performed. After irradiation the post-test analysis phase was performed with the aim to interpret the collected data during operation and dedicated tests and to compare them with the predictions. This paper summarizes the main results of the post-test analysis (PTA), in the three different areas: (1) operational experience and components behavior, (2) thermal hydraulics, and (3) neutronic and nuclear assessment. This analysis was performed as part of the DEMETRA domain of the EUROTRANS IP of the European 6th Framework Program.

The MEGAPIE target (Fig. 1) consisted of a loop of lead–bismuth eutectic (LBE) inside a structure arranged vertically over a length of about 5 m [2,3]. In order to operate the loop, several components were needed. In fact, nine separate components were built separately and then assembled. From bottom to top they were the following: (1) the lower liquid metal container, made of T91 steel. The bottom part was the 1.5 mm thick hemispherical beam window; (2) the lower target enclosure, a double walled, $D_2O$ cooled hull made of $AlMg_3$; (3) the main flow guide tube (316L), representing the barrier between the rising and down coming LBE flow; (4) the central rod, inserted in the LBE, close to the proton interaction

* Corresponding author.
*E-mail address:* luca.zanini@psi.ch (L. Zanini).

0022-3115/$ - see front matter © 2011 Elsevier B.V. All rights reserved.
doi:10.1016/j.jnucmat.2011.04.037

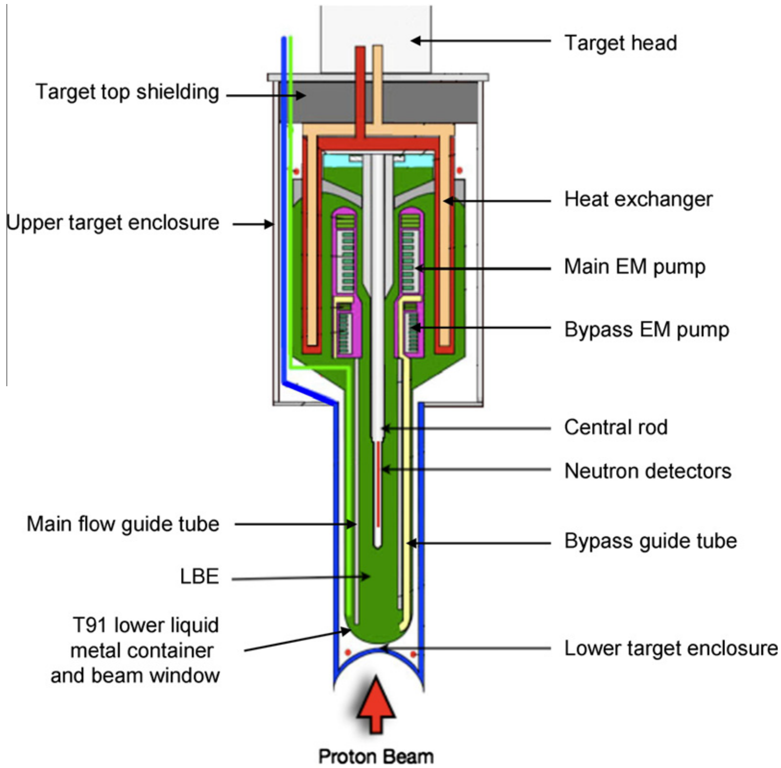


**Fig. 1.** Schematic view of the MEGAPIE target assembly with the main components indicated.

zone, containing heaters and the neutron detectors for flux measurements; (5) the upper target enclosure; (6) the target heat exchanger (THX); (7) the electromagnetic pumps for the main and bypass flow path; (8) the target top shielding; (9) the target head, the upper component of MEGAPIE through which instrumentation lines are fed.

The proton beam penetrated the target from below via two windows. Both the LBE and the structural materials (in particular the beam windows) needed to be cooled. The lower target enclosure was cooled by a forced convection heavy water flow. The inner beam window was cooled by the LBE flow. The lower target enclosure and the beam window were separated by an insulating gap. The LBE flow was provided by two electromagnetic pumps [4]: an axis-symmetric main flow down an annulus (placed between the main flow guide tube and the lower liquid metal container) and an additional flow via a by-pass tube. The combination of main flow and by-pass flow ensured the cooling of the beam window.

The main MEGAPIE ancillary systems directly necessary for the target operation are the heat removal system (HRS), the cover gas system (CGS), the insulation gas system (IGS) and the fill and drain system (F&D) (see Ref. [3] and references therein). The target cooling was one of the most important aspects of the target system design; it was carried out with a triple-loop, three-fluid circuit: the primary LBE loop, an intermediate cooling loop (ICL) filled with oil (Diphyl THT) and a water cooling loop (WCL) to reject the heat in the SINQ main cooling loop. The heated LBE flowed upward through the guide tube to reach the THX where it was cooled and, afterwards, returned to the pump. In the THX the heat was transferred to ICL. The WCL was used to cool the Diphyl oil.

## 2. MEGAPIE operation

The irradiation of the MEGAPIE target started on August 14, 2006. A start up phase at low proton currents, lasting a few days, was followed by the irradiation phase at full power. The peak current reached during irradiation was of 1.375 mA. Irradiation ended on 21 December 2006 (Fig. 2). The main target and irradiation parameters are listed in Table 1.

The MEGAPIE experiment was successful: the target was preheated, filled with LBE, operated 17 weeks with proton beam and then cooled and frozen. The most important procedures related to the operation are discussed in Ref. [5]: filling of the target with LBE; operating; freezing of the target after the experiment. The behavior of practically all the target components was good or, at the least, acceptable. Sometimes some operation problems were faced, but these problems were not serious enough to stop the experiment.

During the target operation in SINQ we observed (Fig. 2): about 5800 proton beam trips of durations less than 1 min; 570 transients with durations of more than 1 min; 1290 steady state beam-on periods longer than 30 min and one steady state period of almost 8 h. After the short beam trips the beam was ramped up slowly, manually by the operator during 20–40 s. During irradiation the temperature in the beam entrance window (BEW) rose from about 230 °C (beam off) to about 300 °C (beam on).

During the MEGAPIE irradiation, several measurements were performed to monitor the target operational parameters, such as temperature, level detection, flow rates and pressure measurements. The instrumentation consisted in the following: (1) level detectors, based on heated thermocouples. (2) oil and water leak detectors, based on the same principles; (3) thermocouples, to ensure target operation and provide temperature measurements for scientific analysis; (4) pressure sensors in the cover gas; (5) leak detectors for the LBE. The most important function of the thermocouples was ensuring the target control during operation. Therefore, the system was not optimal for the target performance scientific analysis. For instance, at the temperature of 300 °C the maximum measuring error ran to 5.4 °C, entailing considerable uncertainty in the target thermal balance. As for the target dynamic

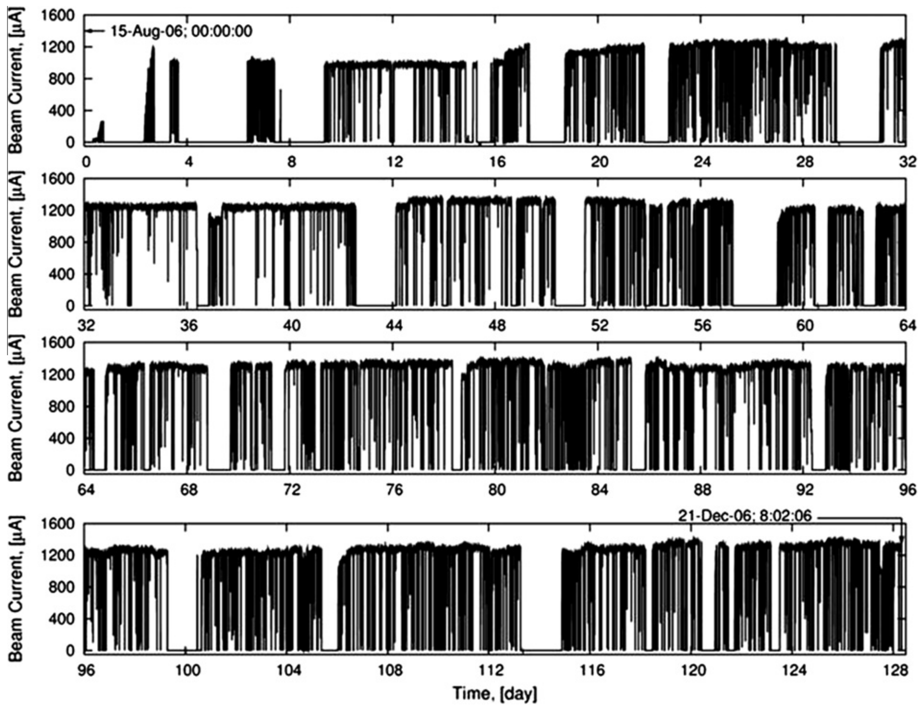


**Fig. 2.** MEGAPIE irradiation history (beam current vs. day of irradiation) from 15 August 2006 until 21 December 2006.

**Table 1**
Main parameters of the MEGAPIE target and of the proton beam.

| | |
|---|---|
| *Main specifications* | |
| Length | 5.35 m |
| Diameter lower part | 10.6 cm |
| Diameter upper part | 20 cm |
| LBE volume | About 87 l |
| *Structural materials* | |
| Lower liquid metal container | T91 steel |
| Upper container | 316L steel |
| Lower target enclosure | $AlMg_3$ |
| *Operation parameters* | |
| LBE temperature range | 230–380 °C |
| Max LBE flow velocity | 1.2 m/s |
| Window temperature range | 330–380 °C |
| *Beam characteristics* | |
| Proton beam energy | 575 MeV |
| Repetition rate | 51 MHz |
| Maximum proton current | 1.375 mA[a] |

[a] Maximum value during MEGAPIE operation.

behavior, the system allowed to analyse processes with a time constant of about 10 s (for instance, the performance of the three-way control valve could be analysed). Another source of uncertainty in the temperature measurements was the location of some thermocouples in places where the temperature gradients in LBE were considerable.

During operation we faced the failure of one of the pressure sensors in the cover gas system. From the beginning indications of the sensors measuring the cover gas pressure were similar, then became more and more different and after about 2 months one sensor failed. An industrial pressure sensor was chosen, modified to avoid problems connected with radiolysis of oil: the membrane was extracted and the oil filling volume between the membrane and a sensing element was removed. The sensor prototype was tested under $\gamma$ irradiation (1 MGray dose) during the commissioning of the target components. Taking into account this experience, it is desirable to look for a radiation hard industrial sensor or to develop a irradiation-hard pressure sensor for a future target.

The performance of the THX and HRS was good. The main drawback of the HRS of MEGAPIE was that it operated with oil. This required the application of the fire safety equipment, consisting in reduction of the oxygen fraction in the target head enclosure chamber (TKE) and compensation of air leakage into the TKE by continuous flushing with nitrogen. An additional problem was the handling of the HRS components contaminated with radioactive oil.

## 3. Main results from the post-test analysis

### 3.1. Thermal hydraulics

#### 3.1.1. Code verification

The THX was an assembly of 12 individual cooling pins inserted into 12 separated channels on the primary side, arranged in semicircles in the upper target (Fig. 3). A three-way valve is located in the oil loop to avoid a strong temperature fluctuation during transients. The experiment has provided data on the thermal–hydraulics behavior of the cooling system to support the validation of RELAP5 (version mod3.2.2β), the ENEA reference system code for transient and safety analysis of LBE and lead cooling systems. The code, which was used by PSI in the design phase to simulate the behavior of the target cooling system at different operational and off-normal conditions, was first assessed in the single-pin tests in Brasimone and in the (MIT) MEGAPIE Integral Tests [6]. In order to correctly predict the thermal exchange in the oil side of THX (LBE-oil target heat exchanger), where exchange conditions are improved by means of a spiral welded on the pipe wall, the Gnielinski correlation [7] has been implemented in RELAP5. These correlations extensively tested for curved ducts have allowed reproducing the steady state conditions of the MEGAPIE cooling system with good agreement. Results for the steady state comparison are shown in Table 2.

In order to verify the RELAP5 code in transient conditions, we selected a beam interrupt event lasting a sufficient time to influence

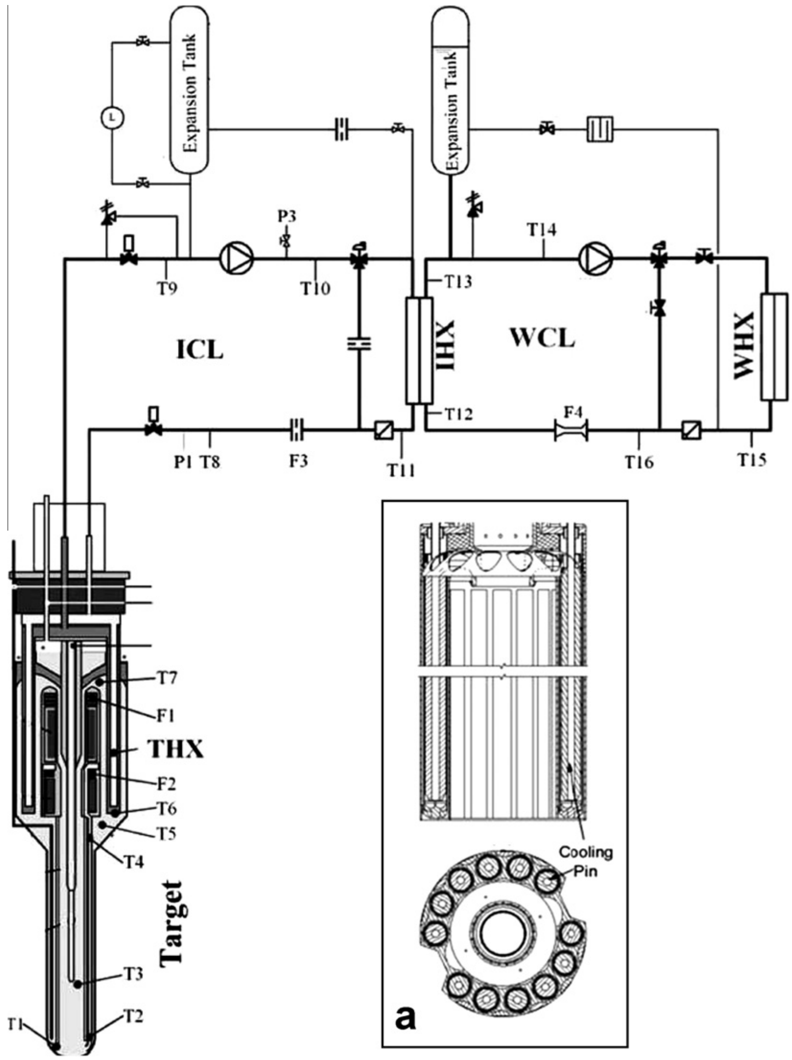


**Fig. 3.** Section of the THX in the upper target (box "a") and scheme of the MEGAPIE cooling system with location of the instrumentation.

**Table 2**
Comparison between measurements and calculations for the MEGAPIE cooling system reference steady state.

| Target power 540.3 kW | | Exp. | RELAP5 standard | RELAP Gnielinsky |
|---|---|---|---|---|
| THX LBE | Mflow (kg/s) | 41.23 | Imposed | Imposed |
| | T1 (inlet) °C | 319.6 | 316.2 | 316.2 |
| | T2 (outlet) °C | 229.5 | Imposed | Imposed |
| THX oil | Mflow (kg/s) | 9.25 | Imposed | Imposed |
| | T3 (inlet) °C | 185.8 | 175.4 | 185.3 |
| | T4 (outlet) °C | 212.9 | 203.5 | 212.6 |
| Ihx oil | Mflow (kg/s) | N.A. | 2.93 | 2.72 |
| | T5 (inlet) °C | 214.4 | 204.1 | 212.9 |
| | T6 (outlet) °C | 112.0 | 109.4 | 110.7 |
| IHX water | Mflow (kg/s) | 8.04 | Imposed | Imposed |
| | T7 (inlet) °C | 33.8 | Imposed | Imposed |
| | T8 (outlet) °C | 49.3 | 50.3 | 50.1 |

the thermal–hydraulic behavior of the cooling loop in a significant way. Calculated temperature trends in Fig. 4 show the good capability of the model to predict the thermal hydraulic response of the circuit. In particular, the three-way valve control, simulated in the code by means of a proportional-integral component, reacts to the LBE temperature decrease with a realistic delay. An underestimation of the heat capacity of the target loop that brings to a faster cooling of the LBE in the THX component can explain slight discrepancies in the decrease of LBE and oil temperatures.

### 3.1.2. Lower target thermal hydraulics

During the MEGAPIE post irradiation examination (PIE) phase the behavior of the structural materials of the target will be examined. One of the main parameters in this investigation is the temperature

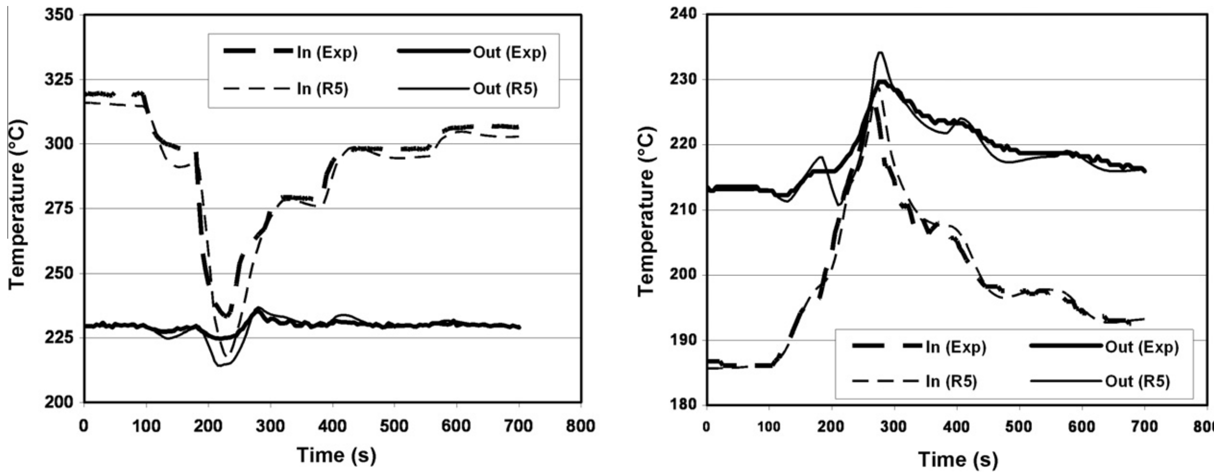


**Fig. 4.** Experimental and calculated (Relap 5) THX LBE and oil temperatures.

of the materials during irradiation. Direct measurement of these material temperatures is not practically feasible but the numerous thermocouples in the lower target region provide already some rough estimation on temperatures in specific regions. (CFD) Computational Fluid Dynamics calculations are then used to extrapolate these readings to temperatures in the positions of the extracted samples. It is therefore crucial that the CFD models that were used in the design phase of the project are benchmarked and updated with real measured temperatures of the target.

The numerical computation of the flow in the lower target region was made with Star–CD 3.26 on a grid of 485,000 elements. The standard $k$–$\varepsilon$ model was employed to simulate steady state turbulent flow conditions. Applying the model as such yielded an underestimation by 10–30 °C of the temperatures at the different measuring points. Consequently, several tracks were considered and tested to explain this discrepancy.

Fig. 5 (left) shows the location of the thermocouples of interest for the lower target. On the right the temperatures extracted from the thermal field at the MEGAPIE thermocouple locations are shown. Temperatures are plotted as a function of their azimuth $\theta$ with the nozzle as the origin. The resulting diagram is a signature of the temperature field in the lower target. Apart from getting rather homogeneous temperatures in the riser, differences between measurements and predictions are observed: the most important difference is that the predicted level is about 10 °C too low in the riser, but 20–30 °C too low at the flow guide edge, except for the inner lateral TCs.

The increase of the heat bypass between riser and down comer to at least 160 kW, compounded by the increase of the mixing temperature at the top of the down comer, obviously contributes to reduce the initial underestimation of the temperature level in the lower target. The exact assessment of the target heat exchanger mean outlet temperature would require a CFD model of the whole LBE circuit and not only of the lower two meters, in order to account for the 3D flow and temperature distributions on the target heat exchanger primary side. Additionally, it was shown how flaws or lacks of the present modeling, like overestimated thermal mixing in recirculation zones by the $k$–$\varepsilon$ model, or suppression of bleed flow through the slots at the flow guide edge, can explain the measurements of the thermocouple lateral sets. Lastly, due to their installation at the edge of irradiated zones with high radial temperature gradients, some bending of the thermocouple end along the direction imposed by the flow would also act in reducing the discrepancies with the prediction. But considering the rigidity of the thermocouple sheaths, this remains hypothetical and would need to be checked by a specific post irradiation examination. Another parameter affecting the thermocouple reading may simply be heat deposition in their metallic sheaths at the edge of the spallation zone that can only work in favor of a local temperature increase, unseen by the nozzle or riser thermocouples.

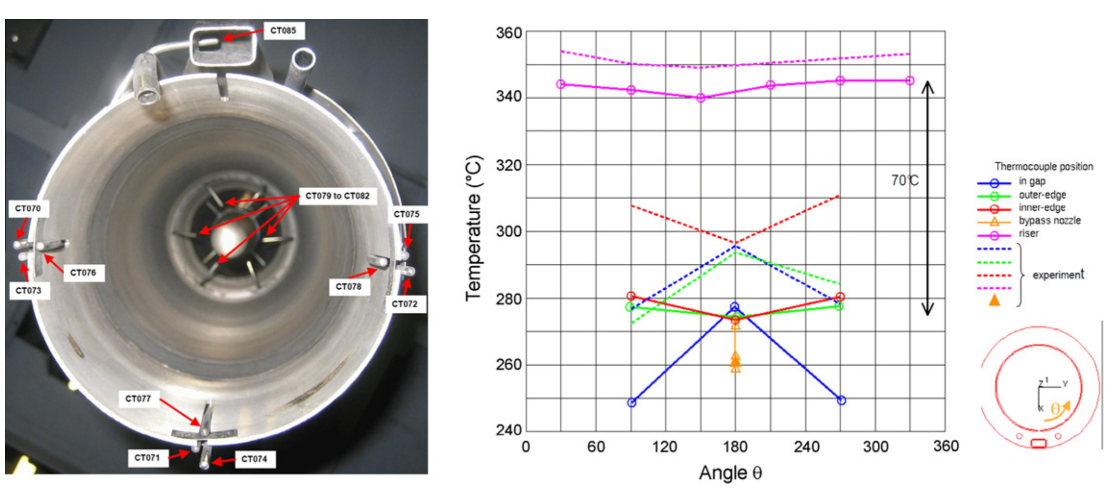


**Fig. 5.** *Left*: picture of the bottom part of the MEGAPIE target without LBE, with indicated thermocouples. *Right*: thermocouple measurements and calculations.

### 3.1.3. Target heat exchanger performance

The heat transfer performance of the THX, ICL and WCL heat exchangers affect the operating conditions of the target. During the pre-irradiation test of the system it was found that the THX is more effective than expected due to an enhanced heat transfer on the coolant side. Therefore, the operating temperature of the ICL is about 50 °C higher than the design temperature. The THX (Fig. 6) consists of 12 separated pins arranged into two semicircles in the upper target. Each pin consists of a straight channel on the primary (LBE) side, and helical annular channel on the secondary (Diphyl THT) side. The helical flow is produced by a guidance which is called the coil below.

In order to investigate the heat transfer performance of the THX for various operating conditions and to aid the post-test analysis of the operating data, Computational Fluid Dynamics (CFD) was used to investigate the thermal–hydraulic behavior of the single cooling pin shown in Fig. 6. The effect of the manufacturing tolerances, which are necessary for assembling, on the heat transfer was studied. In particular the tolerances may lead to an eccentricity when assembling the THX. The eccentricity can affect the heat transfer since the flow field in the THX is changed.

A 3D computational model was set-up. As shown in Fig. 6, the gap width between the coil and pin outer tube (Gap A) was varied in order to investigate effects of eccentricity on the flow field and the average heat transfer coefficient at the heated surface of the cooling pin. Investigated geometries may represent real situations that can occur during assembling of the pin.

Two pairs of cyclic (periodic) boundary conditions model both main and by-pass flow streams (Fig. 6b). The eccentric gap between the coil and the pin outer tube is shown in Fig. 6c. The outer surface is the heated wall (no slip, constant heat flux, $q$ = 260 kW/m$^2$). For both pairs of cyclic boundary conditions A and B (see Fig. 6b) equal pressure drop ($\Delta p$ = 10 k Pa) is prescribed. All other surfaces are adiabatic no-slip walls.

The STAR–CD code was used to predict velocity fields and heat transfer coefficient in the single cooling pin module. A structured mesh with mesh enrichment near solid boundaries was used. The geometrical parameters of the gap between the coil and pin outer tube were systematically varied in order to investigate effects of the bypass flow, coil eccentricity and gap size on heat transfer performance of the cooling pin. Simulations performed with the Low Reynolds number $k$–$\varepsilon$ model show existence of both recirculation and stagnation zones in the main flow stream. Even though oil velocities in the gap (the bypass flow) are higher, the contribution to the overall heat transfer enhancement is smaller as the surface for heat transfer is much smaller. On the other hand large recirculation zones may locally enhance the heat transfer coefficient. The average heat transfer coefficient is calculated based on the following equations: $h_i = \dot{q}/(T_{w_i} - T_{f_i}); h_A = \Sigma_i h_i \cdot A_i / \Sigma_i A_i$, where $T_{w_i}$ is wall temperature, $T_{f_i}$ is fluid cell temperature away from the wall and $A_i$ is cell area. The results presented in Fig. 7 as a function of the Reynolds number show that the heat transfer is enhanced on average.

This sensitivity study illustrates complex thermal–hydraulic behavior of the cooling pin that may affect the performance of THX and the operation of the target.

### 3.1.4. Temperature control performance

The MEGAPIE control system was equipped with a PID loop to control the temperature of the target. Based on the LBE temperature at the exit of the target heat exchanger the position of a control valve in the secondary oil circuit was commanded to maintain a fixed LBE temperature of 230 °C. The position of this valve in the oil loop determined the amount of heat that was extracted from the target.

The target temperature control was designed to keep the temperature of the LBE in the target as constant as possible during normal operation as well as under the influence of fast beam transients in which the full beam power of 600 kW was instantly switched on or off. Analysis of the operational temperature data indicates that during steady operation the target temperature could be controlled within ±2 °C. In periods of low beam power

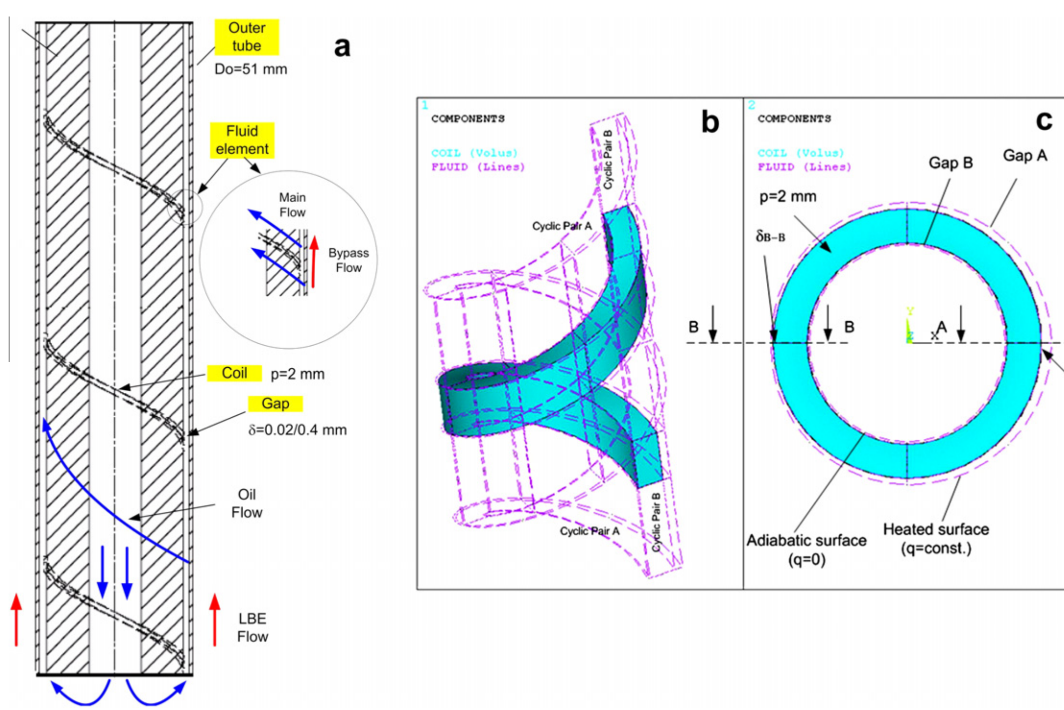


**Fig. 6.** (a) Cross-sectional view of the THX showing helical flow channel. Note: tolerances ($\delta$) are up to 20% with respect to the channel width (p) and (b and c) 3D computational model (*b*: isometric view, *c*: top view). The dashed contours represent the fluid domain and the shaded region represents the coil which has been enlarged for better illustration. Gap A is the gap between coil and pin outer tube, whereas gap B is the gap between coil and pin inner tube (not considered here). The eccentricity $e$ is defined as: $\delta = (\delta_{A-A} + \delta_{B-B})/2$; $e = (\delta_{A-A} - \delta)/\delta$.

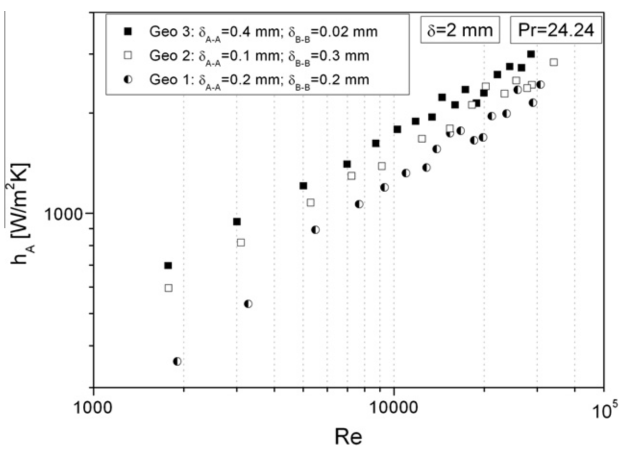


**Fig. 7.** Heat transfer coefficient vs. the Reynolds number for three geometrical configurations. The Prandtl number for the Diphyl THT is of 24.24.

or during hot-standby, small temperature fluctuations could be seen. More detailed analysis suggested that these fluctuations were caused by friction inside the control valve in the oil loop that was used to control the amount of heat extracted from the target. This valve friction introduced a highly non-linear behavior into the control loop which caused these oscillations.

During normal beam trips of 20 s, temperature excursions of maximum 10 °C were recorded. Sporadic temperature excursions up to 20 °C were found when a beam interrupt of a specific time interval occurred. However, these excursions were limited in time and the target integrity was never endangered.

In conclusion, the temperature control system operated satisfactory at keeping the LBE temperature at the target window at a constant predefined level of 230 °C.

### 3.2. Neutronic and nuclear measurements

A series of neutronic and nuclear measurements were performed during the irradiation of the MEGAPIE target. The set of data collected, and the corresponding simulation program carried out allowed to study several neutronic and nuclear aspects, some peculiar to the SINQ facility, others of more general interest to high-power liquid metal targets: (i) characterization of the SINQ facility with the MEGAPIE target from the neutronic point of view; (ii) knowledge of the neutron flux inside a spallation neutron source; (iii) comparison of the neutronic performance of the liquid metal target MEGAPIE with the ones of the solid targets used routinely at SINQ; (iv) measurement of the delayed neutrons; (v) study of the gas release from the target during irradiation; (vi) validation of the Monte Carlo transport codes. Concerning the last point, the experimental work was accompanied by a comprehensive simulation program where the spallation targets and the surrounding SINQ facility were described in great detail, using two state-of-the-art particle transport codes such as FLUKA 2006.3b [8] and MCNPX 2.5.0 [9]. These codes were also used to calculate the activation of the target, or interest for the target disposal and for the PIE.

#### 3.2.1. Neutron fluxes

The spallation source of an ADS must be highly efficient to drive the subcritical core. While it is outside the scope of the MEGAPIE experiment to measure the neutron yield of a spallation target, by measuring the neutron fluxes at several points of the target and of the surrounding facility it is possible to study the neutronic behavior of the spallation source. This can be done by measuring neutron fluxes close to the neutron production zone and at the existing beam lines. This allows validating the transport codes used in the target design, which is essential for further ADS development.

It must be noted that contrary to an ADS, the measured neutron spectra at the SINQ beam lines are mostly thermalized, due to the presence of the large heavy water moderator surrounding the SINQ target. Thermal and epithermal fluxes were measured using gold and cobalt foils at three beam ports at the exit of the SINQ target block, and at the Neutron Activation Analysis (NAA) irradiation station (Fig. 8). Results for the integral fluxes between 0 and 1 eV are shown in Fig. 8 (right). Results are compared with two SINQ solid targets, one irradiated before MEGAPIE (target 6) and one after (target 7). A description of the solid target is found in [10]. The ratio between the measured integral fluxes with MEGAPIE and with the SINQ solid targets 6 and 7 indicate the increase of the neutronic performance using the MEGAPIE target. There is also good agreement between calculated and measured absolute fluxes [11]. Similar results are obtained for the epithermal component which was estimated using gold foils with and without Cd shield. These results indicate that the liquid metal target can produce a considerably higher flux than a solid one. This however depends also on the configuration of the solid target, and in our case the lower performance of the solid targets is mainly due to the amount of heavy water present inside the targets for cooling purposes, that reduces the amount of spallation material. A recent, more optimized solid target irradiated since 2009 has a better neutronic performance than the older ones, thus reducing the gap with MEGAPIE.

The conventional flux measurements with activation foils were complemented with flux measurements inside the spallation target. These challenging measurements were accomplished using micrometric fission chambers inserted in the central rod of the MEGAPIE target. These innovative detectors have been designed and developed [12,13] to provide an on-line measurement of the neutron flux inside the target with accuracy better than 5%. Fission chambers were imbedded in pairs along the axis of the detector over a 50 cm length. Each pair, except one, was made by a chamber containing a $^{235}$U deposit and a chamber without deposit to compensate the fission signal from leakage currents or from currents induced by radiation fields. The bottom pair was shielded with natural metallic Gd (200 μm thickness) to absorb thermal neutrons and be sensitive to epithermal neutrons. Finally, one pair consisted of a chamber with $^{241}$Am and the other one with $^{237}$Np to probe their incineration rate. These different configurations were chosen to provide an overall characterization of the inside neutron flux, in terms of its intensity but also its energy distribution. To increase the accuracy on the energy spectrum determination, nine activation foils were put inside the detector, between the first and the second chamber pairs, in a small titanium box (1.4 cm long and 6.5 mm in diameter). These foils were made by ultrapure metal disks or powder. They provided an integral measurement of the thermal and epithermal flux by capture and threshold reactions.

The current measured by the fission chambers is proportional to the fission rate $\sigma\phi$ which depends on the neutron flux and on the effective fission cross section of the fissile isotope. The extraction of the neutron flux is therefore not straightforward and requires a good characterization of the neutron energy distribution, which was calculated with MCNPX. If the epithermal/thermal ratio does not evolve over time or with the beam intensity, the fission rate is a good estimate of the relative variations of the neutron flux. From the comparison of the experimental and calculated fission rates a systematic over-prediction of the measured values by a factor of 2–3 was found. The fission chamber measurements are in very good agreement with results from activation foils inserted in close proximity. The full data analysis including deep sensitivity studies is in Ref. [14].

The fact that the experimental absolute fluxes at the exit of the target block are well reproduced by the simulation indicates that

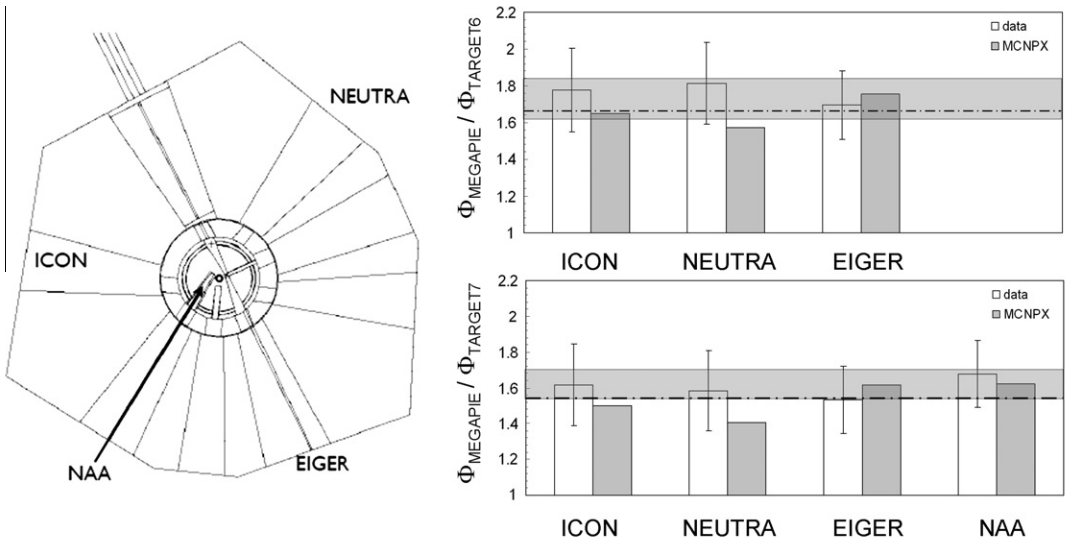


**Fig. 8.** *Left*: XY view of the MCNPX model used in the calculations with indicated positions of the facility where neutron fluxes were measured. *Right*: ratio of the integral thermal fluxes ($0 < E < 1$ eV) between MEGAPIE and the two solid targets, target 6 and target 7. The gray band represents the averaged ratio from the data (1.74 ± 0.12 relative to target 6, 1.62 ± 0.08 relative to target 7). The dot-dashed lines are the average values from the calculations.

overall, the absolute neutronic performances of the targets in the SINQ installation should be correctly calculated. However, significant discrepancies are found in close proximity to the beam interaction zone, i.e., in a region where measurements are more sensitive to the ingredients of the codes to calculate the angular and energy neutron emissions. It will be important for future investigations on high-power liquid metal targets, to understand the origin of these discrepancies as it is directly connected to the neutron production.

### 3.2.2. Delayed neutrons

Another aspect of the neutron flux study that needs to be considered is the delayed neutron (DN) flux. DNs are obviously important in reactors, but they can also constitute a safety issue in high-power liquid metal targets. The reason is that, while in the spallation zone the DN flux is negligible compared to the prompt neutron flux, in other areas of the target loop, where the prompt neutrons are shielded, their contribution might be dominant, both in terms of absolute flux and of energy spectrum. That can be important for instance for ancillary components, which must be qualified also to withstand potentially high DN fluxes.

In order to verify the estimations of the DN flux at MEGAPIE a measurement at the top of the target head was performed. The neutron detection was performed by a 45 cm long $^3$He tube counter installed in a polyethylene box. The $CH_2$ box ensured the moderation of neutrons in order to increase the neutron detector efficiency. The $CH_2$ box was surrounded by a 1 mm thick $^{nat}$Cd foil to avoid the background due to the thermal neutrons. The detector was placed on the floor of the target head enclosure chamber (TKE), at around 3 m from the target head. The interpretation of the data is non-trivial since we do not know *a priori* which precursors are contributing to the DN flux. On the other hand, DNs were measured using 1 GeV protons interacting with massive Pb and Bi targets of variable thicknesses at PNPI Gatchina (Russia) [15]. During this experiment it was found that, contrary to the conventional six-group approach, DN decay curves could be described by four exponential terms corresponding to four dominant isotopes. In particular, up to 10–20 s, major DN contributors come from light mass products, resulting from the spallation process, as $^9$Li and $^{17}$N, rather than fission products as in the case of actinide fission. For longer decay times, from 50 to 100 s, the DN activity is dominated by usual fission products such as $^{88}$Br and $^{87}$Br. This result has been a starting point for the MEGAPIE data interpretation.

In Fig. 9 the measured absolute counting rate of the $^3$He detector (counts/s) normalized to 1 mA primary proton beam current is compared to the calculated one. The black curve shows the equivalent theoretical calculation, which combines DN yields and decay parameters extracted from the PNPI experiment, MCNPX simulations for DN transport from different LBE loop locations to the $^3$He detector position and the calculated $^3$He detector efficiency. The theoretical curve underestimates the experimental data by a factor of 2. The blue curve presents a slightly different scenario, in which one assumes that the LBE was irradiated longer at the proton–LBE interaction point, namely for about 1 s instead of the nominal 0.5 s. In this case, the data are perfectly reproduced. Indeed, in the interaction zone close to the target window, the average LBE speed can be somewhat decreased by vortex formation and the irradiation time can be longer than 0.5 s.

The results from the measurements performed during the MEGAPIE start up confirm that at the top of the MEGAPIE target, the absolute DN flux is comparable to the prompt neutron flux, of the order of $10^6$ n/cm$^2$/s/mA.

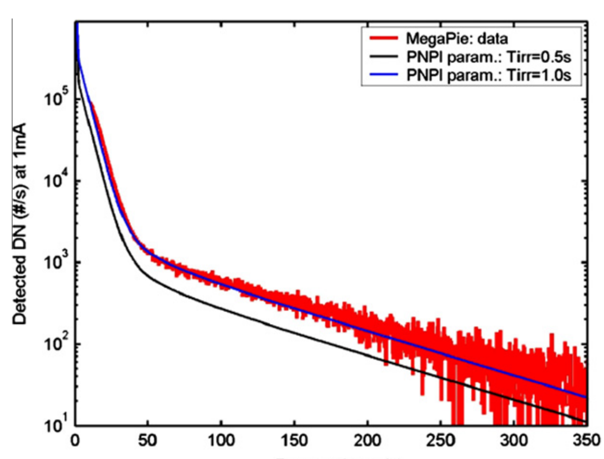


**Fig. 9.** Comparison of measured DN spectrum with two calculations, performed with different transit times of the LBE in the proton irradiation zone.

*3.2.3. Gas production*

The production and release of volatile elements during irradiation is a key safety issue in an accelerator-driven system. One of the main disadvantages of an ADS with respect to a fast reactor system is in the amount of volatile elements ending in the cover gas system (CGS), due to the fact that the coolant is directly irradiated by a proton beam, and a large amount of gas is generated by spallation reactions. This requires special care and makes the handling of the gas more complicated. A large program of calculations and experiments was performed in the frame of the MEGAPIE project to assess the volatility of elements such as noble gases, mercury, and polonium in the MEGAPIE configuration. The complete analysis is given in Ref. [16], while preliminary results are shown in Ref. [17]. In the irradiation phase, absolute amounts of released noble gases and of Hg and Au isotopes were determined by the $\gamma$ spectroscopy measurements from a gas sampling made after 2 days of operation. It was found that only a fraction of the noble gases produced in the LBE was released into the expansion volume after 2 days of operation: the estimated release $f$ of noble gases was obtained by comparing the measured amounts with the calculated ones

$$f = \frac{1}{N}\sum_{i=1}^{N}\frac{m_{i,data}}{m_{i,calc}}, \tag{1}$$

where the sum is over all the noble gas isotopes $N$. The release factor was $f \approx 0.02$. For mercury we can only put a lower limit to the release of $f \geqslant 2.1 \times 10^{-7}$.

It is interesting to plot the mass distribution of calculated and measured amounts of radioisotopes. In Fig. 10 the calculated masses are multiplied by the release factor $f$ for noble gases. In the calculations, FLUKA and MCNPX were coupled with the evolution codes ORIHET [20] and CINDER'90 [21], respectively, to calculate the radionuclides masses corresponding to the experimental irradiation history. From Fig. 10 it is apparent that the fractional release is nearly the same for Ar, Kr and Xe isotopes, indicating a similar release mechanism for all the noble gas elements. One notable discrepancy is found with SNT for the calculated yield of $^{41}$Ar, which is much lower than the value obtained with the other codes. This value results from the use of the improved Fong model [22,23] used in the CASCADE/ASF calculation. The model predicts the sharp decrease of the fission yields for lead and bismuth isotopes with decrease of the fragment mass for $A < 43$. The data obtained for MEGAPIE could be applied for further model improvement.

We know from previous measurements at ISOLDE that noble gases diffuse slowly in LBE targets and the diffusion time decreases as the temperature increases [24]. As expected, the release of Hg was a small fraction of the total, while only traces of Po isotopes were detected from the gas samples, and the amount detected was compatible with decay from the parent astatine nuclides (much more volatile than Po at the MEGAPIE operating temperatures).

A comparison was performed also with expected release rates during the regular gas samplings. In this case the amount of calculated radioisotopes are close to the experimental values, indicating, as expected, that the noble gas release is more complete after 1 month of operation or more.

Unfortunately it was not possible to measure directly hydrogen and helium isotopes. Only indirect measurements, from the pressure in the cover gas, were performed and the calculated pressures compared fairly well with the measured ones.

## 4. Recommendations to liquid metal and ADS target development and conclusions

*4.1. Operation*

The operation of the MEGAPIE target was successful for the whole duration of the irradiation. MEGAPIE was a prototypical target, with possible further development for ADS targets and for general heavy liquid metal target development, including a possible liquid metal target for routine irradiation at SINQ. From the results of the post-test analysis it is possible to make recommendations for an improved and more reliable target for the SINQ facility, and in many cases the recommendations might be extended to ADS development, even though the boundary conditions for a future ADS target will be different than those for the MEGAPIE target developed for SINQ.

Some conclusions and recommendations concerning the pump system can be drawn in the framework of the design of a new liquid metal target for SINQ:

– An electromagnetic pump is the proper mover for a liquid metal target with operation temperature up to 400 °C. The MEGAPIE experiment showed that the pump is liable to operate in the target hot side, submerged in liquid metal under considerable temperature fluctuations caused by the proton beam transients. However, that requires a complicated design protective hull able to withstand the thermal stresses and shortens the life time of the pump. Therefore, it is desirable to find a possibility to place a pump downwards from the THX, where the liquid metal temperature is lower and more stable.

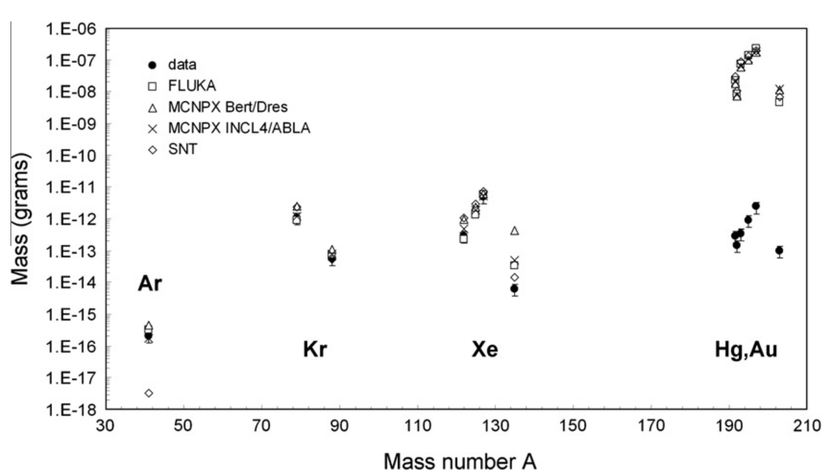


**Fig. 10.** Mass of radioisotopes measured in a sample from the MEGAPIE cover gas shortly after start up. Data are compared with various calculations with FLUKA, MCNPX and SNT [18,19]. Observed Au radioisotopes come from Hg decay. See explanation in the text.

– A new target could be equipped with only one, main flow, electromagnetic pump. A flow structure ensuring proper cooling of the BEW shell and proper mixing can be obtained by optimizing the geometry of the flow area. That makes the target considerably cheaper and reliable.

Additional general recommendations are the following:

– It is desirable to avoid oil as medium for an intermediate cooling loop, and the corresponding fire safety equipment. Possible alternative solutions could be direct water cooling of LBE or via an intermediate liquid metal loop.
– Our operation experience showed that heated thermocouples are not a good choice for leak detectors. Fluctuations of the target temperature connected with beam trips complicate considerably the interpretation of the leak detectors signals.
– Thermocouples of diameter 2 mm with insulated thermal junction are a good solution for the target. They are reliable (no failures or malfunctions during the operation time occurred in MEGAPIE), and accuracy and response times are acceptable for the target control. However, for scientific measurements it is better to foresee special thermocouples, faster reading and more precise.

Finally, some important recommendations come from the analysis of the operation of the gas systems:

– Gas monitoring and sampling are very important and should be performed in a more accurate way, especially to observe the heaviest elements that can be trapped by the system and only partially released. Gas sampling is not a simple operation, and if possible it should be performed remotely; the potential deposition in the CGS pipes of heavy radioisotopes such as Hg might increase the dose rates near the CGS.
– Light gases are the greatest contributors to the pressure build up in the target cover gas system. In the experiment one of the pressure transducers failed during operation, and this shows the importance of having more measuring devices for a reliable measuring system.
– Leaks of radioactive Xe isotopes produced in the LBE were detected in the insulation gas system, corresponding to roughly 1% of the amount of the total inventory in the CGS. The issue of leaks between target components should be carefully studied in future ADS designs.

### *4.2. Thermal hydraulics*

The large set of thermal hydraulic data gathered during the operation of MEGAPIE has been compared to the predicted performance of the target. The existence of some discrepancies between experimental and computational results opens an opportunity for improving both theoretical models and experimental techniques in order to better predict the system behavior and to better instrument the operational facilities. For instance, a reliable prediction of the temperatures in the BEW, which cannot be instrumented with thermocouples, is an important issue for the PIE. The improved computational models and procedures increase the reliability of the methods that will be used for future heavy liquid metal systems and spallation targets development.

The post-test calculations showed the good capability of the RELAP5 code to simulate the thermal hydraulics of the cooling circuit during the MEGAPIE normal operation. In steady state all temperatures, which were predicted by the RELAP5 model of the loop, are in good agreement with the experimental values. Some minor discrepancies in the computation of the LBE temperatures and in the simulation of the oil–water heat exchanger performance have been exhaustively explained. Moreover, the applicability of the code to the transient conditions has been positively verified against an accelerator trip event, thus confirming the conclusion achieved in the previous work on the integral test thermal–hydraulic analysis.

Concerning the detailed 3D computation of the lower target, it is concluded that the difficulty to better match the measurements with calculations not only stems from the inevitable flaws of the turbulence modeling, but also result from the uncertainties on several crucial input data: thermal conductivity of LBE, exact position of thermocouples in hot operation, assessment of a temperature profile at the down comer inlet, exact distribution of the heat deposition – including in the very thermocouples – and heat loss through the guide tube. Any progress in the knowledge or assessment of these factors should help reduce the discrepancy with measurements below the present 10 °C.

The heat transfer performance of the THX, ICL and WCL heat exchangers affects the operating conditions of the target. As during the pre-irradiation test of the system it has been found that the THX is more effective than expected, CFD was used to check the possibility of having enhanced heat transfer on the coolant side. Flows through narrow gaps, annular or leakage flows, and flows through restricted passages are very sensitive to changes in the flow area. Phenomena related to flow-induced vibrations, flow-excited acoustic resonances and heat transfer enhancement and/or reduction are serious design issues encountered in many engineering applications and therefore must be thoroughly considered, especially during design phase of spallation targets. The heat transfer performance of the THX, which depends on the manufacturing tolerances, influences the thermal hydraulics of the lower target since the LBE temperature is affected due to enhanced cooling in THX.

### *4.3. Neutronics and nuclear*

A big effort was devoted to the study of the neutron fluxes in the MEGAPIE target and in the surrounding SINQ facility. The most relevant results are the following:

– Absolute fluxes were determined at different points in the facility, and results have been compared with calculations, obtaining in general an agreement within 20% for thermal fluxes.
– For the first time, the measurement of the neutron flux inside a liquid metal target was performed. Such a system is very important as an online monitor to determine the absolute fluxes and their variations close to the proton interaction zone. A disagreement with calculations of a factor 2–3 (depending on the chamber position) exists. We think that the measurements are correct, since they agree with the results from the flux monitors placed in the same positions. It is likely that the calculations of the fission rates in that particular position are not correct, possibly due to strong flux gradients and to the inherent difficulty of reproducing the mixed neutron spectrum, with large thermal, epithermal and fast components at the detector locations.
– The flux measurement performed in different years at various points of the SINQ facility allowed for a relative comparison of the neutronic performance of the different targets. On the average from four measurement points, MEGAPIE has a neutronic performance higher than target 6 of a factor of $1.74 \pm 0.12$. The performance changes between the two different solid targets and MEGAPIE has been correctly reproduced.

The knowledge of the neutronic performance of an ADS system is a very important parameter, which depends on the spallation target used. From the experience gained in the MEGAPIE work, we learned that this knowledge can be difficult to achieve. Throughout this work it was found that significant changes in the results were usually obtained with each progressive refinement of the geometry, of the materials and of the source definition. In particular, in an attempt to reproduce the experimental results on flux calculations we have progressively refined the description of the geometry of the structural materials in the target and in the SINQ facility. The target and the collimation systems, as well as the structure at measurement points such as the NAA or the fission chambers are relatively complex and are therefore a challenge for the correct modeling of the facility. The correct definition of the structural materials, as well as the precise geometrical definition, is essential in the code validation process.

We think that our studies have confirmed the importance of the DN issues in an ADS, and in liquid metal targets in general. In the particular case of MEGAPIE the DN flux at the top of the target is of the same order of the prompt neutron flux, that is of the order of $10^6$ n/cm$^2$/s/mA. The situation might be different in other target designs, but it is important to consider the delayed neutrons for safety reasons and for the irradiation resistance of the materials (such as detectors or sensors).

The gas measurements provided a large mount of information. Results relevant to the target operation have been discussed in Section 4.1. There are two types of implications to ADS: scientific results gave precise indications of which elements are released during operation, and of the relative release rates of noble gases and mercury isotopes. Gas production measurements by $\gamma$ spectroscopy led to important information on the gas release process in an ADS target. We can summarize the main results:

- noble gas release is a slow process in a real size liquid metal spallation target: the release rates of noble gases in the MEGAPIE system are at the 1% level after 1–2 days of operation, while the release becomes almost complete weeks after the beginning of operation;
- the fractional amounts of the released noble gases are the same for all the elements;
- the mass distributions of the released nuclides can be well reproduced by calculations;
- the release of mercury elements is presumably much lower than the noble gas release, although only a lower limit could be given with our measurement procedure;
- traces of polonium and iodine isotopes were detected from the gas samples. The quantity of Po observed is compatible with production from the decay of parent astatine isotopes, which have higher volatility than polonium;
- pressure increase in the cover gas could be fairly well (within a factor of 2) reproduced with calculations. Given the leaks detected, and the fact that the pressure transducers did not function well during the whole irradiation period, it is a satisfactory result.

In future targets, the sampling should be performed in a more accurate way, especially to observe the heaviest elements that can be trapped by the system and only partially released. Furthermore, it is important to develop a reliable measurement system also for the light noble gases. Additional information on the isotopes produced in the LBE will be obtained in the PIE, from the analysis of LBE samples extracted at various locations of the frozen target.

## Acknowledgments

The authors would like to acknowledge the MEGAPIE initiative and all financing institutions. This work was also supported by the European Community under the IP-EUROTRANS Contract No FI6 W-CT2005-516520. We are grateful to the PSI personnel for the great support given during installation, irradiation and post-test analysis.

## References

[1] G.S. Bauer, M. Salvatores, G. Heusener, J. Nucl. Mater. 296 (2001) 17.
[2] T. Kirchner et al., MEGAPIE target design and dimensioning, in: C. Fazio, J.U. Knebel, F. Gröschel (Eds.), Proceedings of the 4th MEGAPIE Technical Review Meeting, Paris, France, March 18–19, 2003, p. 5.
[3] C. Fazio et al., Nucl. Eng. Des. 238 (2008) 1471.
[4] S. Dementjev, F. Groeschel, N. Jekabsons, Magnetohydrodynamics 44 (3) (2008) 279.
[5] S. Dementjev et al., MEGAPIE-SINQ Experiment. Operational Experience, Components Behavior, PSI Internal Report MPS-SINQ-DS34-102/3.
[6] P. Meloni et al., in: Proceedings of the 10th OECD NEA Information Exchange Meeting on Actinide and Fission Product Partitioning and Transmutation, OECD/NEA, Mito, Japan, 2008.
[7] V. Gnielinski, Int. Chem. Eng. 16 (1976) 359.
[8] A. Fassó et al., FLUKA: a Multi-Particle Transport Code, CERN-2005-10, INFN/TC_05/11, SLAC-R-773, 2005.
[9] D.B. Pelowitz (Ed.), MCNPX user's Manual Version 2.5.0, LA-CP-05-0369, 2005.
[10] G.S. Bauer, Y. Dai, W. Wagner, J. Phys. IV France 12 (2002).
[11] S. Panebianco et al., Ann. Nucl. Energy 36 (2009) 350.
[12] S. Chabod et al., Nucl. Instrum. Methods A566 (2006) 633–653.
[13] A. Letourneau et al., in: Proceedings of the International Conference ANIMMA, Marseille, France, IEEE 2009, in press.
[14] F. Michel-Sendis et al., Nucl. Instrum. Methods B 268 (2010) 2257.
[15] D. Ridikas et al., Eur. Phys. Journ. A 32 (2007) 1–4.
[16] N. Thiolliere et al., Nucl. Sci. Eng. (2011), accepted for publication.
[17] L. Zanini et al., Neutronic and Post-test Analysis of MEGAPIE, PSI Report 08-04, ISSN 1019–0643, December 2008.
[18] Yu.A. Korovin, A.Yu. Konobeyev, P.E. Pereslavtsev, Voprosy Atomnoi Nauki I Techniki (Problems of Nuclear Science and Technology), Series: Nuclear Data 3 (4) (1992) 117.
[19] A.Yu. Konobeyev, Yu.A. Korovin, M. Vecchi, J. Nucl. Sci. Technol. (Suppl. 2) (2002) 1256.
[20] F. Atchison, H. Schaal, Orihet 3 – Version 1.12, A Guide for Users, March, 2001.
[21] W.B. Wilson, T.R. England, A Manual for CINDER'90 Version C00D and Associated Codes and Data, LA-UR-00-Draft, 2001.
[22] P. Fong, Phys. Rev. 135B (1964) 1338.
[23] A.Yu. Konobeyev, Yu.A. Korovin, M. Vecchi, Kerntechnik 64 (1999) 216.
[24] Y. Tall et al., in: Proceedings of the International Conference on Nuclear Data for Science and Technology, Nice, 2007, p. 1069.